Multilevel Fault Detection and Diagnosis on Office Building HVAC Systems

Siyu Wu and Jian-Qiao Sun, University of California at Merced

ABSTRACT

This paper presents a multilevel fault detection method. Two key features of the proposed method are 1) an energy description of all the units in a HVAC system and 2) a spatial-temporal partition approach, which allows us to apply the FDD strategy to the entire building in a uniform manner. Energy flow models for HVAC units at all levels are presented. The concept of absolute and relative references for monitoring the energy performance is introduced. A numerical example of cross-level fault detection involving an upper level AHU and lower level VAVs is presented where a fault from the AHU is detected. With the limited real time data, we discuss the threshold for detecting this AHU fault. More measurements and extensive studies are needed to establish thresholds for various faults at different levels.

Nomenclature

E	energy flow density
ΔE	energy flow density change across HVAC units
E_{AH}	energy consumption of AHU
E_{VS}	sum of energy consumption of VAVs
C_v	specific heat capacity of flow at constant volume
T	flow temperature in degree K
T_S	supply flow temperature
T_D	discharge flow temperature
T_E	exhaust flow temperature
T_R	return flow temperature
T_O	outside air temperature
ρ	flow density
v	flow velocity
v_S	supply air velocity
v_E	exhaust air velocity
v_R	return air velocity
v_O	outside air velocity
V_S	supply air volumetric velocity
V_E	exhaust air volumetric velocity
V_R	return air volumetric velocity
V_O	outside air volumetric velocity
A	cross section area of the AHU terminal
D_E	damper position of the exhaust air duct
D_R	damper position of the return air duct

Introduction

Buildings represents one of the fastest growing energy consuming facilities on the earth. According to the U.S. Department of Energy 2009 Building Energy Data Book, buildings use 72% of nation's electricity, 54% of natural gas and 38.9% of nation's total energy consumption, valued at $392 billion (U.S. Department of Energy 2009). Heating, ventilating, and air conditioning (HVAC) system is an indoor environmental technology which has been widely equipped in modern buildings. The three central functions of heating, ventilating, and air-conditioning are interrelated, providing human comfort and acceptable indoor air quality. Currently, HVAC accounts for 57% of the energy used (valued at $223 billion) in U.S.

commercial and residential buildings, and the industry employs around 1.1 million people. Unfortunately, HVAC may fail to meet the performance expectations due to various faults, poor controls and improper commissioning, thus wasting more than 20% energy it consumes (Roth et al. 2005). Therefore, it is of great potential to develop automatic, quick-responding, accurate and reliable fault detection and diagnosis (FDD) schemes to ensure the normal operations of HVAC in order to save energy. According to the National Institute of Standards and Technology (NIST), FDD methods have a potential to save 10-40% of HVAC energy consumption (Schein et al. 2006). A FDD package for HVAC can help to establish construction and renovation standards for new and existing buildings. In light of the worldwide energy crisis and increasing environmental awareness, and the current limited usage of renewable energy in buildings, FDD for HVAC is critical to increase the energy efficiency in buildings.

Existing FDD methods can be divided into two categories: statistical method and computational model based approaches. The statistical methods implement fault detection algorithms to analyze current conditions in comparison with past normal conditions. Schein et al. developed 28 rules to detect 5 typical faults in the air handling unit (Schein et al. 2006). Seem used robust estimates of the mean and standard deviation to detect abnormal energy consumption in buildings (Seem 2007). Wang and Xiao applied principal component analysis (PCA) to detect sensor fault in AHU (Wang and Xiao 2004; Xiao and Wang 2009). By setting proper threshold learned from trainings, Du et al. detected flow sensor fault in air dampers and VAV terminals (Du et al. 2009). Hoyle studied the PCA dimension selection for high dimensional data and small sample sizes (Hoyle 2008).

The computational model based approach calculates and predicts the normal operations based on computational simulation of the HVAC system. The prediction forms the basis for fault detection. Clarke et al. developed a simulation-assisted control to simulate and test the response of building energy management systems (BEMS) (Clarke et al. 2002). Pedrini et al. applied the EnergyPlus simulation tool to develop a methodology for monitoring the energy performance of a commercial building in Brazil (Pedrini et al. 2002). Researchers from Lawrence Berkeley National Laboratory have been working on Modelica and EnergyPlus simulation tools for years (Wetter 2009). Djuric et al. reviewed the possibilities and necessities for building lifetime commissioning and estimated the heating system performance using optimization tool and BEMS data (Djuric and Novakovic 2009). Namburu et al. developed a generic FDD scheme for centrifugal chillers and a nominal data-driven model of the chiller to predict system response (Namburu et al. 2007). Haves et al. investigated the model-based performance monitoring in chillers (Haves and Khalsa 2000).

All the existing classical FDD methods are level or hardware dependent. There is room for improvement to achieve a system level FDD. In particular, there is a need to develop methods for detecting faults across different levels of the HVAC system with a focus on energy consumption of the system. The proposed method should be computational efficient and less onerous from a calibration perspective compared to most computational model based approaches. This paper develops a FDD method with these features.

The rest of the paper is organized as follows. In Section 2, we present the basic idea of the proposed multilevel FDD method with the direct consideration of energy consumption. In Section 3, we use PCA as an example of the methods of analysis to demonstrate how to apply the proposed method. Section 4 presents a numerical example of the FDD with the real monitored data from a building on campus of the University of California at Merced.

Multilevel FDD Algorithm

Two key elements of the proposed method are 1) an energy description of all the units in a HVAC system, and 2) a spatial-temporal partition strategy. A uniform model to describe dynamics of units at different levels is a starting point of the multilevel FDD algorithm. Since the ultimate goal is to reduce energy consumption, we choose energy flow density across a unit to describe its dynamics. The energy model is certainly applicable to all the units. We can use the monitored sensor data to estimate energy performances of all HVAC units at different levels. These signals are the input to the FDD algorithm. In this work, we shall investigate if the energy model can capture hardware faults within the HVAC system.

Environmental factors of rooms in a building such as sun exposure and local wind direction strongly influence the energy needs for cooling and heating. Human and architectural factors, such as floor level, room function, and occupancy conditions also demand different levels of energy consumption. Temporal factors, such as seasonal changes and day and night switch, change the control sequences and setpoints, thus impacting the energy consumption. All of these factors form a basis for dividing rooms as well as VAVs into subgroups. The units in a subgroup share more common factors, have stronger correlations, and may be monitored with a same set of thresholds for fault detection. FDD studies make use of a high dimensional matrix consisting of real-time measurements of the HVAC components, interior and exterior temperatures, occupation sensors, etc. The spatial and temporal grouping of the units essentially provides a physics-based partition of the matrix for more effective analysis.

Energy Flow Model

We consider energy transfer and consumption of hardware units at different levels. The boiler or condenser supplies the building with heating and chilling water. The pump transfers the water. The variable frequency drives (VFD) fan produces pressure difference to supply air. The energy supplied to the HVAC system is eventually converted to water or air flow with a certain temperature and velocity. A HVAC unit can be simplified as a blackbox with input and output flows shown in Figure 1.

Figure 1: Units at Different Levels of HVAC can be Treated as Blackboxes with Input and Output Flows of Air or Water with Certain Temperatures, Velocities and Densities

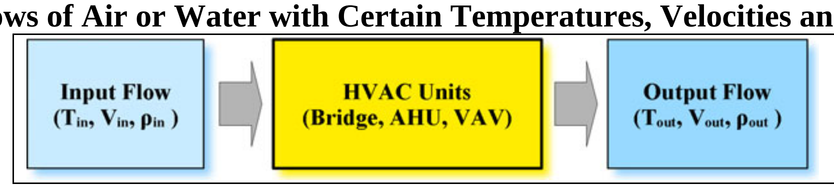

The energy density of the flow through a blackbox can be written as

$$E = C_v T + \frac{1}{2}\rho v^2 . \qquad (1)$$

It is reasonable to assume that C_v is a constant, the input flow rate is the same as the output air because of the continuity condition. To compute the energy consumption of a unit with known geometry, we need five variables: T_S, T_D, v, C_v and ρ. The C_v and ρ are both known functions of temperature and pressure.

Figure 2: An AHU Unit can be Treated as a Blackbox with Two Inputs and Two Outputs

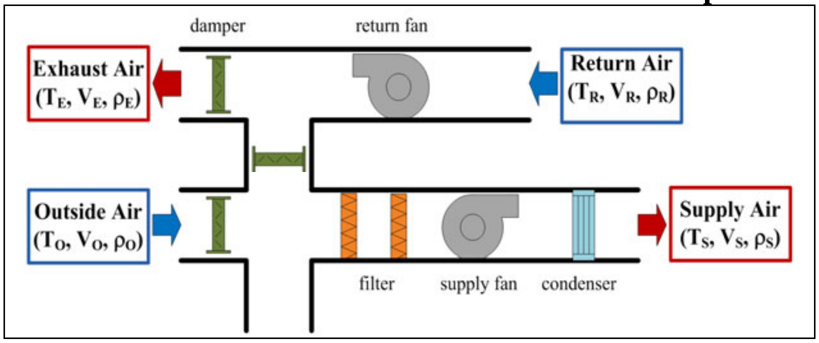

An AHU unit can have two inputs: return air and outside air, and two outputs: supply air and exhaust air as illustrated in Figure 2. The energy flow density change across the AHU is given by

$$\begin{aligned} \Delta E \ &= \ C_v \Delta T + \frac{1}{2}\Delta(\rho v^2) \\ &= C_v(T_S + T_E - T_R - T_O) + \frac{1}{2}\rho(v_S{}^2 + v_E{}^2 - v_R{}^2 - v_O{}^2) \end{aligned}, \qquad (2)$$

where four temperatures involved are part of the original monitored data. The air velocities v_S, v_E, v_R, and v_O are

$$v_i = V_i / A. \qquad (3)$$

The continuity condition of the flow in AHU leads

$$\begin{aligned} V_O &= V_S - \frac{D_R}{D_R + D_E} V_R \\ V_E &= \frac{D_E}{D_R + D_E} V_R \end{aligned}. \qquad (4)$$

From these equations, we arrive at

$$\Delta E \ = \ C_v(T_S - T_O) + \frac{\rho D_R D_E}{D_R + D_E}(V_S{}^2 - V_R{}^2). \qquad (5)$$

The proposed approach directly focuses on the energy consumption of a unit, reduces the number of parameters to monitor, and makes it easier to integrate with a FDD algorithm so that we can treat all the units in a uniform manner.

A special case of the AHU is when the return air damper is completely closed such that $D_R = 0$. The energy consumption density is reduced to

$$\Delta E \ = \ C_v(T_S - T_O) + \frac{1}{2}\rho V_S{}^2. \qquad (6)$$

The AHU is connected to a number of VAVs. A VAV has only one input: the supply air from its upper-level AHU and one output: the discharge air. The supply and discharge air velocities as well as the corresponding air duct geometries are the same. The energy flow density change across the VAV is

$$\Delta E \ = \ C_v(T_S - T_D). \qquad (7)$$

References for Fault Detection

Under steady-state, since the room temperature is almost constant and the return air temperature is nearly the same as the room temperature, the difference between the outside and room temperatures is a driving force of energy consumption of the HVAC system. For a certain temperature difference, the HVAC units should keep a certain level of energy consumption. An unexpected fluctuation above or below this level is considered abnormal. The units with abnormal energy consumption in reference to the outside temperature may be faulty. In this sense, we call the outside temperature as an absolute reference.

To confirm the fault, we compare the energy consumption of the possibly faulty unit with that of other units at the same level or with a mathematically equivalent measure. This comparison provides a relative reference. Specifically, we investigate the correlation between the suspicious unit and other units at the same level or the mathematically equivalent measure. An example of the mathematically equivalent measure is the energy consumption of an AHU and the sum of energy consumption of all its lower-level VAVs.

Principal Component Analysis

There are several methods for analyzing the measurement data for fault detection. In this paper, we use the principal component analysis (PCA) as an example to demonstrate the application of the proposed multilevel FDD method. The PCA is widely used for dimension reduction in pattern recognition. By mapping a set of correlated variables to a smaller set of uncorrelated variables known as the principal components, the PCA can approximately reconstruct the original data based on a new basis formed by the vectors associated with the principal components. The order of the principal components is determined by the variability in the original data (Bishop 1995).

In the analysis, it is more intuitive to keep the data with the same physical attribute together in one matrix. Take image processing as an example. The physical attributes of the matrix are uniform such as brightness and greyness. For the same reason, we compute the energy flow density of HVAC units from the monitored parameters with different physical attributes.

Let $\mathbf{X}^T$ be a data matrix where its rows represent samples of the data, and its columns normalized to have zero mean are observations of all samples. The PCA transformation is given by

$$\mathbf{Y}^T = \mathbf{X}^T \mathbf{W} = \mathbf{V\Sigma}, \quad (8)$$

where $\mathbf{V\Sigma W}^T$ is the singular value decomposition (SVD) of $\mathbf{X}^T$ (Strang 1998).

The PCA reveals the internal correlation structure of the data. If a multivariate data set is considered to represent an object in a high-dimensional space, the PCA provides a low-dimensional projection of the object with the most informative viewpoints along the principal eigen-directions, which are often called “patterns” of the data. We propose to project the principal components a sub-space spanned by the measurements of interest. Since the principal components are calculated from the whole data set in the higher dimensional space, their projections on to the sub-space contain physical interactions with all other measurements.

Figure 3: The Projection of the Dominant Principal Component onto the 2-Dimensional Plane Spanned by Two Measurements M_1 and M_2 of Interest

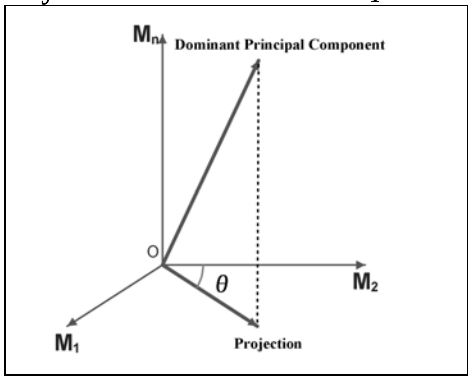

As an example, consider a sub-space spanned by two measurements M_1 and M_2. The projection of the principal component into the sub-space is illustrated in Figure 3. The measurements are related as

$$M_1 = k \cdot M_2, \tag{9}$$

where the slope is $k = \tan\theta$ and θ is the projection angle. When $0 \le \theta \le \pi/2$, M_1 and M_2 are linearly and positively correlated within the principal component. When $\pi/2 \le \theta \le \pi$, M_1 and M_2 are linearly and negatively correlated. We postulate that the projection angle changes with the conditions of the HVAC system, particularly when a fault occurs.

Let θ_n denote the nominal value of the projection angle between the measurements M_1 and M_2 when the system is in normal operational condition. How much deviation of θ from θ_n would signal the existence of a fault? We need a large number of measurement data and various faulty incidents to train an algorithm in order to establish the threshold for θ statistically.

Assume that projections of the principal component suggest that the unit associated with measurement M_k may be faulty. Since only the energy flow density of a unit is used in the analysis, more signals from the unit can be used to further investigate the nature of the fault, which can be due to the failure of fan, motor, and other electrical or mechanical components of the unit. This can be done with the existing FDD methods as reviewed in Section 1.

A Numerical Example

Let us consider an example to demonstrate the procedure of the proposed FDD strategy. We select an AHU (A10) and its 29 lower level VAVs in the HVAC system of the Science and Engineering Building on the UC Merced campus. Figure 4 demonstrates a single VAV's one week temporal plot of data from several available sensors. We use data collected from May 1 to May 28, and June 15 to July 12 in 2009. We remove the trend and normalize the data as

$$\overline{x_i} = \frac{1}{N}\sum_{n=1}^{N} x_i^{\,n},\ \sigma_i^2 = \frac{1}{N-1}\sum_{n=1}^{N}(x_i^{\,n} - \overline{x_i})^2,\ \overline{x_i}^{\,n} = \frac{x_i^{\,n} - \overline{x_i}}{\sigma_i}, \tag{10}$$

where x_i^n represents i^{th} measurement at sample time n. Since the sampling intervals of the original data are not uniform, we reconstruct the data matrix by using samples only on the least common multiples of all the different sampling intervals. We do not apply any interpolation.

Figure 4: One Week Temporal Plot of Sensor Data from a Single VAV Installed on the Target Building on UC Merced Campus

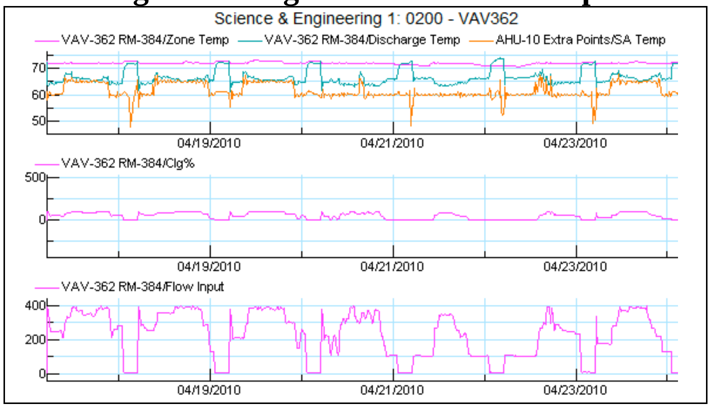

We consider a matrix consisting of three measurements: the outside temperature T_O, the AHU energy consumption E_{AH} and the sum of energy consumption E_{VS} of the VAVs. We apply PCA to this matrix, compute the dominant principal component, and project it onto 2-dimensional planes formed by two of the three measurements.

As a temporal partition strategy, we consider the weekly performance of the system. Figure 5 - 7 show the results of projections of the principal component for the data in June to July. In Figure 5, the projection angles of weeks 1, 2 and 3 are close to each other at nearly 45°. The projection angle of week 4 is far away from that of the other three weeks at nearly 160°. The projection angles of these four weeks are listed in Table 1.

Table 1: Projection Angles on Planes Created by Selected Measurements

Projection Angle	Week 1	Week 2	Week 3	Week 4
$\theta(T_O, E_{AH})$	33.96°	42.66°	43.14°	167.84°
$\theta(T_O, E_{VS})$	48.88°	49.17°	49.19°	41.09°
$\theta(E_{AH}, E_{VS})$	59.55°	51.48°	51.03°	103.88°

From the physics point of view, every pair of the three measurements T_O, E_{AH} and E_{VS} should be linearly and positively correlated. In weeks 1, 2 and 3, the projection angles are near 45° indicating a linear and positive correlation. The projection angle of week 4 is 160° indicating a negative correlation. Figure 5 suggests that during weeks 1, 2 and 3, the AHU behaved normally as its energy consumption is positively correlated with the absolute reference T_O. However, during week 4, a fault may have occurred, which caused abnormal energy consumption.

Recall that the mathematically equivalent measure of the energy consumption of an AHU is the sum of energy consumption of all its lower-level VAVs. Figure 6 shows that the projection angles of all four weeks are in the first quadrant around 45°, which verifies that all the VAVs were functioning normally because the sum of their energy consumption E_{VS} correlates positively with T_O. Hence, the sum of energy consumption of all the VAVs can serve as a relative reference for the AHU. This indirectly confirms the fault detected in Figure 5.

Figure 5: Projection of the Dominant Principal Component from Weekly Observations onto the two Dimensional Plane Spanned by E_{AH} and T_O. Weeks 1-3: Magenta Dashed Line, Blue Dotted Line and Green Dashdot Line. Week 4: Solid Line

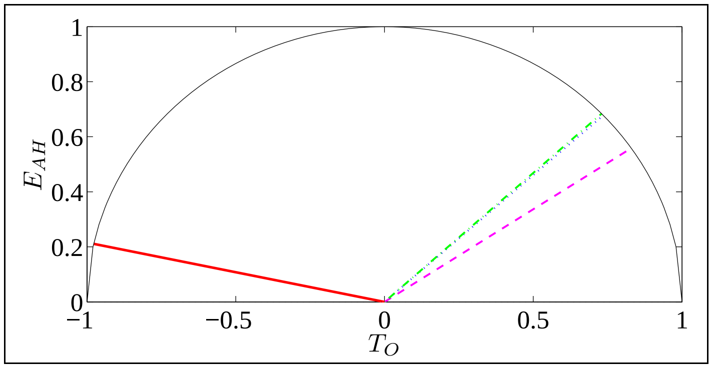

Figure 6: Projection of the Dominant Principal Component from Weekly Observations onto the Two Dimensional Plane Spanned by T_O and E_{VS}. Legends are the same as in Figure 5

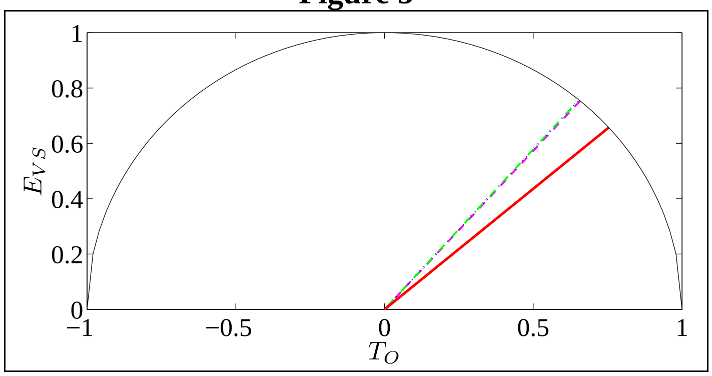

Figure 7: Projection of the Dominant Principal Component from Weekly Observations onto the Two Dimensional Plane Spanned by E_{AH} and the Mathematically Equivalent Measure E_{VS}. Legends are the same as in Figure 5

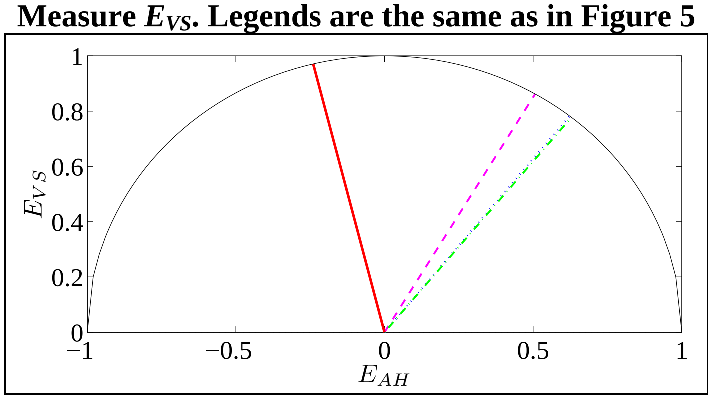

Figure 7 compares the AHU energy E_{AH} with the relative reference E_{VS}. It is clear that the projection angle of week 4 deviates significantly from that of the other three weeks, and confirms the fault occurred in the AHU in week 4.

We have confirmed with the building manager that the supply fan of the AHU was frozen for the entire fourth week in July as shown in Figure 8. Meanwhile the return fan of the AHU was working normally. So it was the frozen supply fan that caused the abnormal energy consumption for the AHU in week 4 recorded in the June-July data set.

Given the knowledge of the fault, let us now try to determine thresholds of the projection angle. We use the data of four weeks in May and first three weeks in June-July data set when the system was under normal condition. We compute the standard deviation of the projection angle, and consider the 90% probability interval of the projection angle $[\bar{\theta}-1.644\sigma_\theta, \bar{\theta}+1.644\sigma_\theta]$ where $\bar{\theta}$ is the average projection angle and σ_θ is the standard deviation. The probability is computed based on the Gauss distribution assumption. We propose to use $\pm 1.644\sigma_\theta$ from the average as the threshold for fault detection.

Figure 8: The Supply Fan Speed of the Monitored AHU (blue solid line) Demonstrates that it was Frozen for Almost the Entire Last Quarter (The Fourth Week) of the Monitored Period in July, While the Return Fan of the AHU (Red Dashed Line) was Functioning Normally. This Confirms the Suspicious Fault We Detected in Week 4 of July

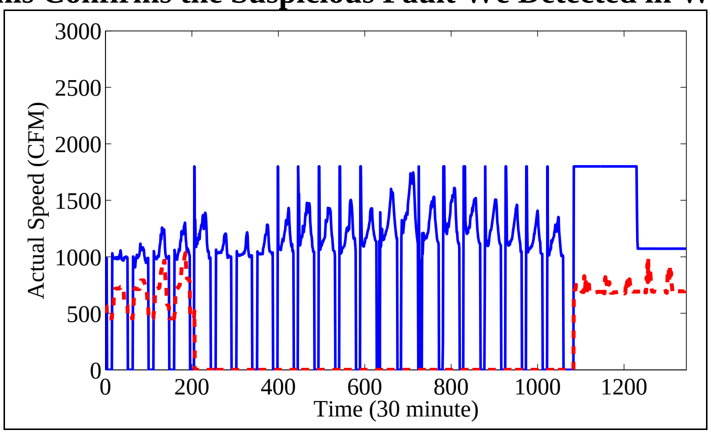

Figure 9 shows the projection angle of weekly observations. It can be seen from the figure that the projection angles of the seven weeks when the system was normal are close to the average value, and the projection angle of week 4 in the June-July data set goes out of the lower boundary of the threshold.

To demonstrate the effect of different temporal partition, we present the same analysis with daily observations in Figure 10. The figure shows a considerable number of samples going beyond the threshold in the last six days, specifically in the first and third subplots where the energy consumption of the AHU is compared with the absolute reference T_O and the relative reference, i.e. the mathematically equivalent measure E_{VS}.

It should be noted that the above discussion on the threshold is limited by the availability of the measurements with known faults, and should not be generalized. Future effort of this research will search for more real time measurements with known faults or generate the data with artificially introduced faults, as is commonly done in the literature.

Figure 9: Projection Angles of the Principal Component of Weekly Observations of 8 Weeks in May to July 2009. The 90% Probability Thresholds with $\pm 1.644\sigma_\theta$ are Marked by Red Dash-Dot Lines with Triangular Symbols, and the Average Projection Angle by Black Dashed Line. Blue Line with Square Symbols Denotes the Actual Projection Angle of the Week. The Plot of the Last Week Indicates a Possible Fault During that Time. This Fault is Verified as the Frozen Supply Fan Shown in Figure 8

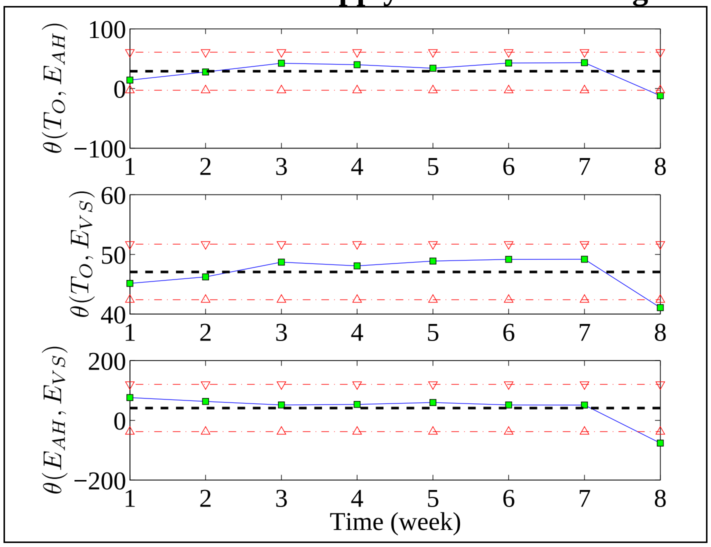

Figure 10: Projection Angles of the Principal Component of Daily Observations of 8 Weeks in May to July 2009. Legends are the same as in Figure 9. Plots Involving E_{AH} Show that the Projection Angles Exceed the Threshold for Three to Four Days in the Last Week Indicating a Possible Fault During that Time. This Fault is Verified as the Frozen Supply Fan Shown in Figure 8

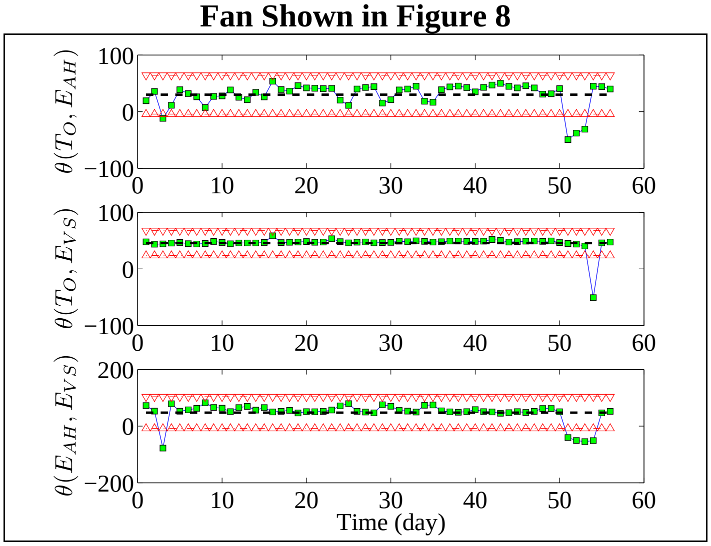

Conclusions

A multilevel fault detection method has been introduced in this paper. Two features of the proposed method, i.e. 1) an energy description of all the units in a HVAC system and 2) a spatial-temporal partition strategy, allow us to apply the FDD strategy to the entire building in a uniform manner. To this end, we have developed energy flow models for HVAC units at all levels. We have discussed the inherent complexity of HVAC systems, and proposed the concept of spatial and temporal subgrouping. The concept of absolute and relative references for monitoring the energy performance has been introduced. A numerical example of cross-level fault detection involving an upper level AHU and lower level VAVs is presented where a fault in the AHU is detected. With the limited real time data, we have studied the threshold for detecting this AHU fault. More measurements and extensive studies are needed to establish thresholds for various faults at different levels.

In the future, we plan to apply the proposed FDD algorithm to all HVAC units at different levels in a building to capture various patterns of energy consumption, and study relationship between energy consumption patterns and dominant principal components. In addition to PCA, other methods of analysis such as the dynamic model decomposition (DMD), correlation analysis, and spectral analysis will be examined in connection to the proposed multilevel FDD strategy with a hope to achieve thresholds of higher accuracy and reveal more details of the system performance patterns.

References

[DOE] U.S. Department of Energy. (2009). "**Building Energy Data Book**." <http://buildingsdatabook.eren.doe.gov/>.

Bishop, C. M. (1995). **Neural Networks for Pattern Recognition**, Clarendon Press, Oxford.

Clarke, J. A., Cockroft, J., Conner, S., Hand, J. W., Kelly, N. J., Moore, R., O'Brien, T., and Strachan, P. (2002). "**Simulation-Assisted Control in Building Energy Management Systems**." *Energy and Buildings*, 34(9), 933-940.

Djuric, N., and Novakovic, V. (2009). "**Review of Possibilities and Necessities for Building Lifetime Commissioning.**" *Renewable and Sustainable Energy Reviews*, 13(2), 486-492.

Du, Z., Jin, X., and Yang, X. (2009). "**A Robot Fault Diagnostic Tool for Flow Rate Sensors in Air Dampers and VAV Terminals**." *Energy and Buildings*, 41(3), 279-286.

Haves, P., and Khalsa, S. K. (2000). "**Model-Based Performance Monitoring: Review of Diagnostic Methods and Chiller Case Study**." *Proceedings ACEEE Summer Study on Energy Efficiency in Buildings*, American Council for an Energy-Efficient Economy, 3161-3171.

Hoyle, D. C. (2008). "**Automatic PCA Dimension Selection for High Dimensional Data and Small Sample Sizes**." *Journal of Machine Learning Research*, 9, 2733-2759.

Namburu, S. M., Azam, M. S., Luo, J., Choi, K., and Pattipati, K. R. (2007). "**Data-Driven Modeling, Fault Diagnosis and Optimal Sensor Selection for HVAC Chillers**." *IEEE Transactions on Automation Science and Engineering*, 4(3), 469-473.

Pedrini, A., Westphal, F. S., and Lamberts, R. (2002). "**A Methodology for Building Energy Modelling and Calibration in Warm Climates.**" *Building and Environment*, 37(8-9), 903-912.

Roth, K. W., Westphalen, D., Feng, M. Y., Llana, P., and Quartararo, L. (2005). "**Energy Impact of Commercial Building Controls and Performance Diagnostics: Market Characterization, Energy Impact of Building Faults and Energy Savings Potential**." TIAX LLC, Cambridge, Massachusetts.

Schein, J., Bushby, S. T., Castro, N. S., and House, J. M. (2006). "**A Rule-Based Fault Detection Method for Air Handling Units**." *Energy and Buildings*, 38(12), 1485-1492.

Seem, J. E. (2007). "**Using Intelligent Data Analysis to Detect Abnormal Energy Consumption in Buildings**." *Energy and Buildings*, 39(1), 52-58.

Strang, G. (1998). **Introduction to Linear Algebra 3rd Edition**, Wellesley-Cambridge Press.

Wang, S., and Xiao, F. (2004). "**AHU Sensor Fault Diagnosis Using Principal Component Analysis Method**." *Energy and Buildings*, 36(2), 147-160.

Wetter, M. (2009). "**Modelica-Based Modelling and Simulation to Support Research and Development in Building Energy and Control Systems**." *Journal of Building Performance Simulation*, 2(2), 143-161.

Xiao, F., and Wang, S. (2009). "**Progress and Methodologies of Lifecycle Commissioning of HVAC Systems to Enhance Building Sustainability.**" *Renewable and Sustainable Energy Reviews*, 13(5), 1144-1149.